

PAPER • OPEN ACCESS

Multi-axis piezoelectric energy harvesting using MEMS components with slanted beams

To cite this article: Pontus Johannisson *et al* 2016 *J. Phys.: Conf. Ser.* **773** 012080

View the [article online](#) for updates and enhancements.

You may also like

- [Varying intercept regression model](#)
Rosalia, S Abdullah and S Nurrohmah
- [Development and Analysis of Electronic and Electrical Experiment Simulation Technology](#)
Liuning Zhu and Chuanwu Liu
- [Decreasing inventory of a cement factory roller mill parts using reliability centered maintenance method](#)
Witanty and Anita Rindiyah



ECS
The
Electrochemical
Society
Advancing solid state &
electrochemical science & technology

DISCOVER
how sustainability
intersects with
electrochemistry & solid
state science research

Multi-axis piezoelectric energy harvesting using MEMS components with slanted beams

Pontus Johannisson, Fredrik Ohlsson, Cristina Rusu

Acreo Swedish ICT AB, Arvid Hedvalls Backe 4, SE-411 33 Gothenburg, Sweden

E-mail: pontus.johannisson@acreo.se

Abstract. During the manufacturing of MEMS components, slanted beams can be produced in the etching process. We show that this can be used to produce skew motion that causes deflection of a proof mass out of the device plane also when the excitation is confined to the device plane. This allows construction of an energy harvester that uses a planar manufacturing process and produces power also with in-plane excitation. To obtain this with traditional methods it would be necessary to manufacture separate components and then mount them with their sensitive axes orthogonal to each other.

1. Introduction

The increasing need to sense and communicate is driven, e.g., by networked devices and sensors in the internet of things. It is often difficult to arrange wired power supply and the use of batteries necessitates regular replacement and disposal. Energy harvesting from vibrations is often considered, converting kinetic energy into electric energy using electromagnetic, electrostatic, or piezoelectric transduction [1]. Energy harvesters (EHs) utilizing piezoelectric materials are most popular and this approach is used in this study.

One common way to implement an EH is as a cantilever with a proof mass at the tip and with PZT in a uni- or bimorph configuration [2]. Regardless of the design choices, a traditional EH generates negligible power when the excitation is in the device plane. One obvious solution is to use more than one EH. Combining three orthogonal EHs it is possible to obtain power regardless of the excitation direction but this requires an extra assembly step, reduces the device compactness, and increases the cost.

In this paper, we consider the use of slanted beams, which can be fabricated by wet etching of silicon. As the etching rate depends on the crystal orientation, planes inclined at $\arctan(\sqrt{2}) \approx 54.74^\circ$ can be produced. Due to this slantedness, an in-plane excitation is partly converted to an out-of-plane deflection and the axis corresponding to the maximum power is rotated from the out-of-plane direction. This method has previously been used to design an accelerometer [3], but to the best of our knowledge this approach is novel in the EH context. Using numerical simulations in COMSOL Multiphysics, we compare our approach to a traditional cantilever EH with a rectangular beam and report how the output power is affected, to what axis it corresponds, and to what extent the device is a multi-axis EH.

2. Design approach

For compatibility with MEMS manufacturing it is assumed that the PZT is deposited on top of the silicon structure. The PZT material, PZT-5H, is assumed to be operated in the 31 mode, i.e., the strain is orthogonal to the electric field. A further choice is to target a relatively low



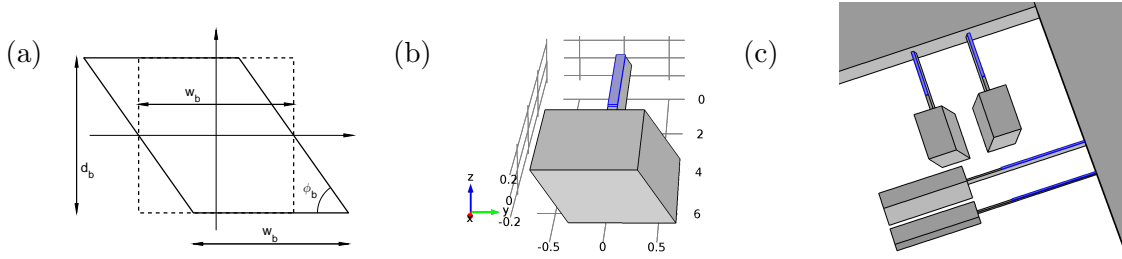


Figure 1. (a) The slanted beam with $\phi_b = \arctan(\sqrt{2}) \approx 54.74^\circ$. In the case with a rectangular beam (dashed line), all angles are $\pi/2$. (b) The slanted beam EH with PZT (blue). A more robust design is discussed in the main text. (c) One possible combination of four EHs.

frequency at 300 Hz. The geometry of the beam is shown in Fig. 1a, both for the slanted (solid line) and rectangular (dashed line) cases, and the beam width, w_b , and thickness, d_b , are defined in the same figure. It is not possible to change only the beam angle as this changes the eigenfrequency of the structure, leading to a drastically different response to a given excitation. Furthermore, the aspect ratio, defined as $\eta \equiv d_b/w_b$, will be varied and this leads to similar problems. Therefore, the first resonance frequency of the different EHs was kept at 300 Hz by adjusting the beam length.

Focusing on the multi-axis potential, the design is kept very simple. We emphasize that other designs that preserve the qualitative features are possible. For example, one approach would be to use two beams offset in the y direction (instead of the x direction) from the proof mass. Attaching one end of the beams to the proof mass and the other to the frame, a robust S-shaped EH is obtained. Here, we investigate the cantilever structure shown in Fig. 1b. The volume of the proof mass is kept constant, although the shape depends on the etching. The proof mass is made of silicon and has the dimensions $3 \text{ mm} \times 1 \text{ mm} \times 0.5 \text{ mm}$, cf. Fig. 1b. The width of the beam, w_b , is selected to be 0.1 mm. When the thickness is varied, the length of the beam is adjusted to keep the first resonance at 300 Hz. The mass and the beam would have their upper surfaces aligned in practice but we here align their centroids for simplicity. The PZT thickness is $20 \mu\text{m}$. It has the same width as the beam and we set the length of the PZT to 3 mm. The electrodes are placed on the top and bottom surfaces of the piezoelectric layer and connected by a $50 \text{ k}\Omega$ load resistance. This is approximately the average of the optimum values for the slanted ($80 \text{ k}\Omega$) and rectangular ($20 \text{ k}\Omega$) cases.

Also an EH with a slanted beam will generate negligible power when the excitation is perpendicular to the sensitive direction. Thus, the intention is to combine four of these EHs as conceptually suggested in Fig. 1c. Note that the beams are slanted in different directions.

3. Numerical simulations

As both the volume of the proof mass and the stiffness (via the resonance frequency) of the beam are kept constant, comparable motion of the proof mass is obtained in all cases. The beam length as a function of the aspect ratio is shown in Fig. 2a. As the length of the PZT is constant, it is not possible to make the slanted beam very thin. Thus, the slanted beam thickness is not made smaller than $70 \mu\text{m}$. In the rectangular case, the beam length increases faster with the beam thickness. The reason for this difference is that when d_b increases for the slanted beam, the weakest direction of the beam is rotated.

The fact that the slanted beam has its weakest direction at an angle makes the aspect ratio an important parameter. When the aspect ratio is increased the weakest direction turns toward the in-plane direction, but at the same time the power is reduced as the strain in the PZT is reduced. The power angular dependence is exemplified in Fig. 2b. In this case, the EH is excited harmonically using body forces. The acceleration amplitude is $1g$ and the frequency is 300 Hz.

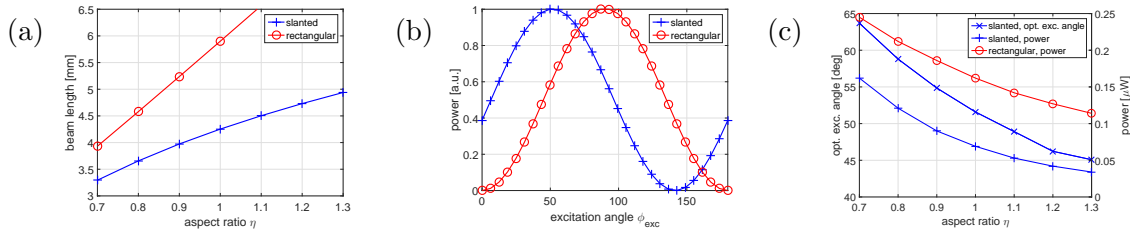


Figure 2. (a) The beam length as a function of the aspect ratio. (b) Example results of the EH power as a function of the excitation direction. (c) The optimal excitation angle and the EH power as a function of the aspect ratio.

The direction of the acceleration is rotated ϕ_{exc} in the y - z plane and the power, normalized to its peak value, is plotted. The rectangular beam has its maximum power for $\phi_{exc} = \pm 90^\circ$, while the maximum for the slanted beam depends on the aspect ratio. In Fig. 2b, $\eta = 1$ has been used. The optimal excitation angle has been plotted as a function of the aspect ratio for the slanted beam (using \times markers) in Fig. 2c. It is seen that for the thinnest slanted beam ($\eta = 0.7$), the optimal excitation angle is largest (64°). If the beam would be made even thinner, the optimal angle would approach 90° . On the other hand, for thick beams the optimal angle is reduced, but the reduction rate is not fast. For very thick beams, with $\eta \gg 1$, the weakest direction of the beam corresponds to $\phi_{exc} = 90^\circ - 54.74^\circ \approx 35^\circ$, cf. Fig. 1a.

In Fig. 2c, the EH power is plotted as a function of the aspect ratio for the slanted and rectangular beams. However, these values were *not* obtained from steady-state solutions with harmonic excitation. The reason is that the damping is very small as the PZT layer is thin. This leads to low electrical losses and very high quality factors. Thus, the power is very sensitive to the exact choice of excitation frequency. In practice, the damping would be dominated by phenomena such as drag forces [4] or squeeze film damping [5]. However, these effects depend on parameters that are not part of the current investigation. Therefore, the time-dependent simulations used an acceleration pulse in the form of a sine wave at 300 Hz truncated after the first period. The energy spectral density of this pulse is obtained from the convolution of the Fourier transform of the sine function and a rectangular window. It has its maximum close to 300 Hz but will not have its energy concentrated at a single frequency. The pulse amplitude is $10g$, but the power with this short excitation is limited to the sub- μ W regime.

Simulations have been performed with this pulsed excitation using the optimal excitation angle according to Fig. 2c. (For the rectangular beam, the excitation angle is $\phi_{exc} = 90^\circ$.) After the pulse, the proof mass is oscillating and, due to the choices in Section 2, the maximum kinetic energy is equal in all cases. The maximum power has been plotted in Fig. 2c. It is seen that the slanted beam gives approximately 66 % of the power with $\eta = 0.7$ and that the relative difference increases with the aspect ratio. This is expected since the rectangular beam gives maximum strain in the PZT.

4. Discussion

To see to what extent the power generation can be made independent of the excitation direction, it is instructive to plot the EH power as a function of the excitation direction, see Fig. 3. As shown in Fig. 2b, the power varies harmonically with the excitation angle. The amplitude varies between zero and the maximum value and the period is π . Thus, the normalized power can be plotted as a function of the excitation angle in an angular plot, where the distance from the origin to the curve corresponds to the normalized power. In Fig. 3a, the case for a rectangular beam is shown. When the angle is zero, the power is zero and maximum power occurs for $\phi_{exc} = \pm 90^\circ$. The slanted beam case can be visualized using Fig. 2c. Assuming that there are

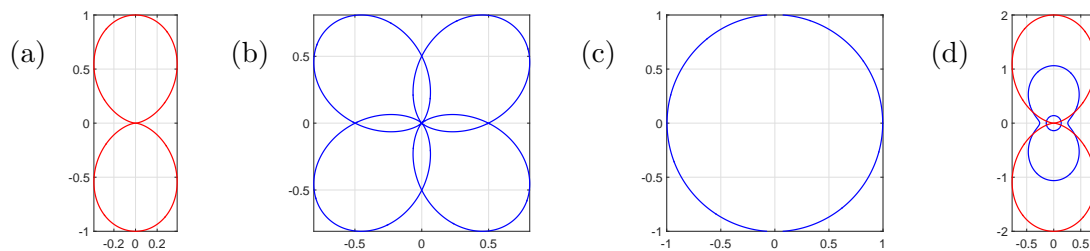


Figure 3. (a) Normalized power lobe for a rectangular EH. (b) Normalized power lobes for two EHs using $\eta = 1.3$ with beams slanted in different directions. (c) The total power for the two EHs in b. (d) Power lobes for two square EHs (red) and two slanted beam EHs (blue) using $\eta = 0.7$ and $\eta = 1.3$, respectively.

two slanted beam EHs (cf. Fig. 1c), there are two lobes as shown in Fig. 3b. The relative angle between the lobes and the absolute power is selected, via the aspect ratio, from Fig. 2c. The optimal excitation angle is $\pi/4$ when the slanted beam $\eta = 1.3$. Using this value would give an isotropic two-dimensional (2D) EH, as the sum of the power from the two EHs is then a circle, see Fig. 3c. However, this is sub-optimal as the power decreases rapidly with increasing aspect ratio. Instead maximizing the power for an in-plane excitation, $\eta = 0.7$ is optimal and the optimal excitation angle is 64° . This leads to the power lobes in Fig. 3d. In red, the power from two rectangular beams is plotted. The inner blue curve is the circle from Fig. 3c with correctly scaled relative power and the outer blue curve corresponds to $\eta = 0.7$. The difference compared to the red curve is due to that (i) the slanted beam EHs redistribute the sensitivity angles and (ii) the slanted beam EHs give 66 % of the power.

The above selection leads to maximum power for an in-plane excitation. Unfortunately, the difference in power comparing the in-plane and out-of-plane excitations is close to a factor of four. To achieve a three-dimensional (3D) system, two additional EHs are needed, cf. Fig. 1c. As the out-of-plane excitation will yield another identical contribution to the power, the power ratio for the out-of-plane and in-plane excitations will then increase to a factor of eight.

5. Conclusion

The potential of using slanted beams in MEMS EHs to obtain power also when the excitation is in the device plane has been investigated. With the current approach, the slanted beam EH gives 66 % of the power but is superior in the sense that it generates power for in-plane excitation. Combining two slanted beam EHs into a 2D harvester, it is possible to obtain constant output power, but when optimizing the EH power for in-plane excitation, there is a factor of four power difference comparing out-of-plane and in-plane excitation. For the cases where the power specification is met also considering this difference, the objective of constructing a planar multi-dimensional EH can be obtained.

Acknowledgments

The Smart-MEMPHIS project has received funding from the European Union's Horizon 2020 research and innovation programme under grant agreement No. 644378.

References

- [1] Harb A 2011 *Renewable Energy* **36** 2641–2654
- [2] Roundy S and Wright P K 2004 *Smart Materials and Structures* **13** 1131–1142
- [3] Rödjegård H, Andersson G I, Rusu C, Löfgren M and Billger D 2005 *J. Micromech. Microeng.* **15** 1989–1996
- [4] Blom F R, Bouwstra S, Elwenspoek M and Fluitman J H J 1992 *J. Vac. Sci. Technol. B* **10** 19–26
- [5] Bao M and Yang H 2007 *Sens. Actuators* **136** 3–27